

Microarticle

Characteristics of an on-chip polariton successively filtered circuit

J. Ali^a, N. Pornsuwancharoen^b, P. Youplao^b, I.S. Amiri^c, R.R. Poznanski^d, K. Chaiwong^e,
S. Punthawanumt^f, S. Suwanarat^g, P. Yupapin^{h,i,*}

^a Laser Centre, IBNU SINA ISIR, Universiti Teknologi Malaysia, 81310 Johor Bahru, Malaysia

^b Department of Electrical Engineering, Faculty of Industry and Technology, Rajamangala University of Technology Isan, Sakon Nakhon Campus, 199 Phungkon, Sakon Nakhon 47160, Thailand

^c Division of Materials Science and Engineering, Boston University, Boston, MA 02215, USA

^d I-CODE, Universiti Sultan Zainal Abidin, 21300 Kuala Nerus, Terengganu, Malaysia

^e Department of Electrical and Electronics Engineering, Faculty of Industrial Technology, Loei Rajabhat University, Loei 42000, Thailand

^f Multidisciplinary Research Center, Faculty of Science and Technology, Kasem Bundit University, Bangkok 10250, Thailand

^g Department of Physics, Faculty of Science, Ramkhamheang University, Bangkok 1220, Thailand

^h Computational Optics Research Group, Advanced Institute of Materials Science, Ton Duc Thang University, District 7, Ho Chi Minh City, Viet Nam

ⁱ Faculty of Electrical & Electronics Engineering, Ton Duc Thang University, District 7, Ho Chi Minh City, Viet Nam



A B S T R A C T

Polaritonic signal processing model and manipulation using a microring successive filtering circuit are proposed. The polariton signals are generated by the coherent light within the microring embedded a gold nanograting island, from which the successive filtering of the polariton signals within the designed on-chip circuit is manipulated by adjusting the device end reflection coefficients. The almost closed system of the two-level system of polaritons is formed, where there are initially two oscillation frequencies called the Rabi frequencies, the ground an excited state respectively. The required signals of this characteristics study are presented in the domains of wavelength, time and frequency, which can be used to characterise the brain signals in the meditation situation. When the successive polariton switching time (Δt) is approaching zero, from which the stopping polariton state is established, while the polariton frequencies can be tunable. The results obtained have shown that switching time of the 2nd successive round-trip of 25.55 fs is obtained, and in addition, the tunable frequencies of the ground and excited states of the two-level system are achieved.

Polariton is a quasiparticle that can be generated by the coupling between the electric dipole and strong field, which is generally found in the plasmonic wave propagation in the medium [1–3]. Polariton is also confirmed that it can be used in brain-like artificial neural network models [4–6], in which the interaction between the signal (photon) and ionic dipole can generate quasi-polariton. Principally, the information among cells and body can be linked to the brain by the polariton transmission line (liquid core waveguide), where which the polariton network is established. Hagan and Hirafuji [7] consider a “psycho-physical” bridge between interfacial water’s molecular dipoles and differing condensates in the quantum realm and the resultant transfer of information between the classical and quantum domains based on a polariton model. By using the polariton approach the artificial neural network signals can connect to the ionic dipole, where the information can be encoded and decoded by the spin-up and down of the quasi-polariton. However, the proposed model present only the hardware part, therefore, the wetware part is required to establish the realistic link. In practice, the liquid core waveguide can be used to establish such

a link through quantum fluids representing the environment of biomolecules in neuronal microstructure of fine distal branchlets [8]. In this work, we consider only the hardware, where the almost closed system of the brain chip is designed using the polariton generation system, where the successive filtering brain signal is model and simulated using the two different programs, which are the Optiwave and MATLAB programs. The device scale and parameters are used close to the real world. The required interpretation will be the meditation behaviors and levels, which are based on the obtained output.

The successive polariton filtering system is as shown in Fig. 1, where light from a monochromatic light with the selected wavelength is used as the input source. The polaritons can be generated by the coupling between the plasmonic grating and the strong electromagnetic field, in which the strong fields can be formed by the coupling light waves between the two nonlinear side rings and center ring. The two side rings are made of the nonlinear materials that can introduce the nonlinear effect into the oscillation output pulse, which results in the shorter switching time and high output power that can be obtained. In this

* Corresponding author at: Computational Optics Research Group, Advanced Institute of Materials Science, Ton Duc Thang University, District 7, Ho Chi Minh City, Viet Nam.

E-mail address: preecha.yupapin@tdtu.edu.vn (P. Yupapin).

<https://doi.org/10.1016/j.rinp.2018.09.021>

Received 9 August 2018; Received in revised form 7 September 2018; Accepted 9 September 2018

Available online 25 September 2018

2211-3797/ © 2018 The Authors. Published by Elsevier B.V. This is an open access article under the CC BY license (<http://creativecommons.org/licenses/by/4.0/>).

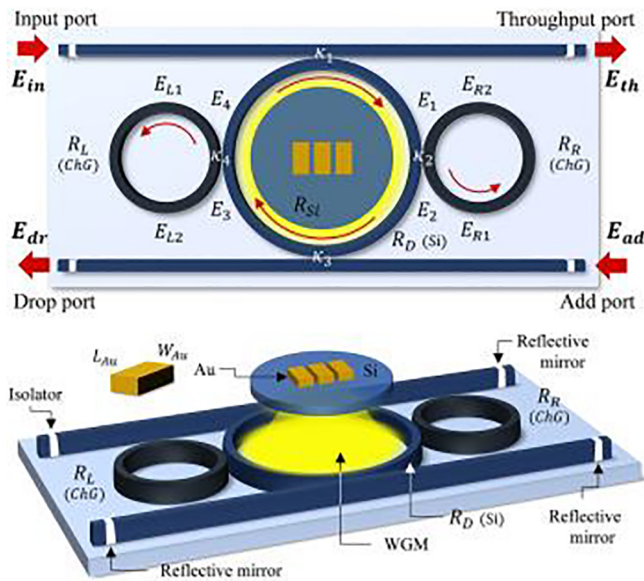


Fig. 1. The system model of the polariton generation using the gold grating embedded in a Panda-ring resonator, where E_{in} , E_{th} , E_{dr} , E_{ad} are the electrical fields of the input, through, drop and add ports, R_R , R_L , and R_D are the right, the left, and the centre rings, respectively, all coupling coefficients are $\kappa_s = 0.5$. R_{Si} : Silicon circle radius, L_{Au} and W_{Au} are the gold grating dimensions.

proposed work, the successive filtering signals can be operated by adding the reflectors on the device ends, which are the gold nano-grating embedded plasmonic island, through, drop and add ports. From which the system is almost a closed system. The used reflector material is the TiO_2 , in which the reflection and transmission power at the add port can be controlled by the material length.

The successive filtering output signal will have the shorter in time than the input signal, which means that the pulse width (Δt) is approaching zero for the long-running successive filtering. Another aspect is that the tunable Rabi oscillation frequency signals can also be obtained by varying the input light source power.

The required output of the successive filtering system is the add port output (I_{add}), which can be obtained by using the following relationship [9].

$$I_{in} = I_{th} + I_{drop} + I_{add} \tag{1}$$

where I_{in} , I_{th} and I_{drop} are the input, through and drop port intensities, respectively.

The input intensity is given by

$$E_{in} = E_z = E_0 e^{-ik_z z - \omega t + \varphi} \tag{2}$$

where E_0 is the initial electric field amplitude, k_z is the wave number in the direction of propagation, ω is the angular frequency [10], where φ is the initial phase.

The add port output of the system in Fig. 1 is given by [11]

$$I_{add} = -R_{WGM} \cdot I_{WGM} \cdot R_{WGM} \tag{3}$$

where R_{WGM} is the reflectance of the applied material, for an examples, gold and TiO_2 . The proposed system was simulated based on practically achievable device parameters which are given in the captions of relevant figures [12]. The reflected grating output signal of the system is shown in Fig. 1, where the reflected light power is entered into the Panda-ring system, where the peak reflection ($P_B(\lambda_B)$) at the waveguide port is approximately given by $P_B(\lambda_B) \approx \tan^2 \left[\frac{N\pi(V)\delta n_0}{n} \right]$ [9,13]. Here N is the number of the periodic variations, δn_0 is the refractive index variation of the waveguide, n is the fraction of power in the waveguide core, and $\Delta\lambda = \left[\frac{2\delta n_0 \pi}{\pi} \right] \lambda_B$.

Principally, the human brain signals are configured as the polaritons

after the coupling between the brain signal (electromagnetic wave) and the ionic dipole [8]. In a meditation, the brain signals can be configured as the polariton successive filtering signals, which can be performed and manipulated by the polariton successive filtering circuit, in which the polariton can be and localised within the closed system (body). The polariton signal oscillation can be configured to be the Cerenkov radiation aspect [15], in which the stopping polariton behavior in time can be established when the change in time is approaching zero, which is the stopping condition [16], which means that the cold system condition of the polariton oscillation within the system can be established, where $1/2 mv^2 = NK_B T$ is satisfied, where m and v are the particle mass and velocity respectively. N is the particle number. K_B is the Boltzmann constant, and T is the absolute temperature. The polariton Rabi oscillation frequencies can be tuned finer and finer, which have the different energy levels. However, the suitable meditation technique is required. Otherwise, the closed system condition may be broken and brought the bad effect. Finally, the polariton field strength is very high because there is no noise affected in this situation, which leads to having the very high brain performance.

In a simulation, the preliminary results are obtained by using the Optiwave program and shown in Fig. 2, where the selected parameters are used and given in the related figure captions. The 2nd filtered loop result is shown in Fig. 3, where the 0.9 reflection coefficient is applied, where the reflected coefficient is 0.9, the oscillation times of ~ 2.6 and 2.55 fs of the 1st and 2nd round filtering are obtained, respectively. The faster switching time of 0.045 fs than the 1st loop is obtained. The increase in the number of successive filtering loop leads the shorter in time is obtained, when delta time is approaching, the stopping condition is formed, where the “cold body”, “slowing in time” and “superconducting” states are established. The simulation results of the polariton in terms of wavelength (frequencies) of the two-level system are obtained at the drop and add ports are shown in Fig. 4, where the ground and excited state frequencies are obtained respectively. The red and blue shifts can be seen, from which the Cerenkov radiation can be formed and the aura state established. In Fig. 5, the simulation results of the system with the same parameters of Fig. 2, where the selected input

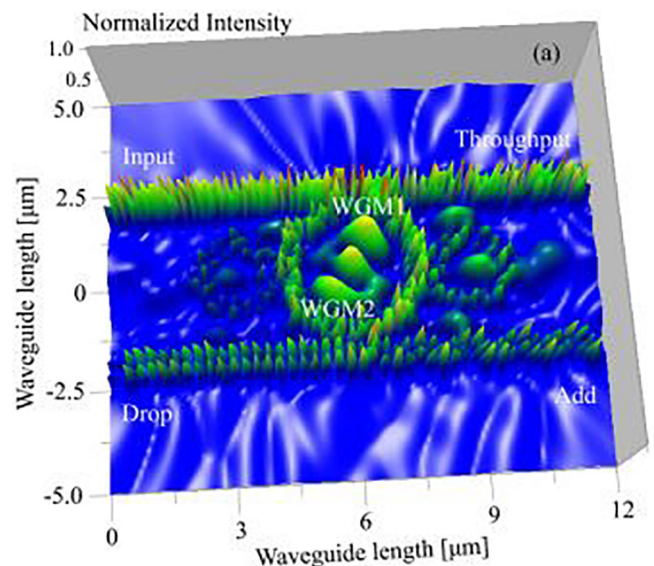


Fig. 2. The results of the polariton oscillation distribution in the system in Fig. 1 using the Optiwave program, where the input light pulse power is 50 mW with the center wavelengths of $1.55 \mu m$. The ring system, $R_L = R_R = 0.8 \mu m$, $R_D = 1.55 \mu m$. All κ_1 to $\kappa_4 = 0.5$, the grating pitch is $0.1 \mu m$. The refractive index; $n_{0ChG} = 2.9$, the nonlinear refractive index, $n_{2ChG} = 1.02 \times 10^{-17} m^2 W^{-1}$ [14], $n_{Si} = 3.47$ (Si-Crystalline silicon). TiO_2 dimensions are $width \times Length \times depth = 0.5 \mu m \times 0.5 \mu m \times 0.2 \mu m$. The used waveguide loss is $0.10 dB cm^{-1}$, the core effective area is $0.30 \mu m^2$.

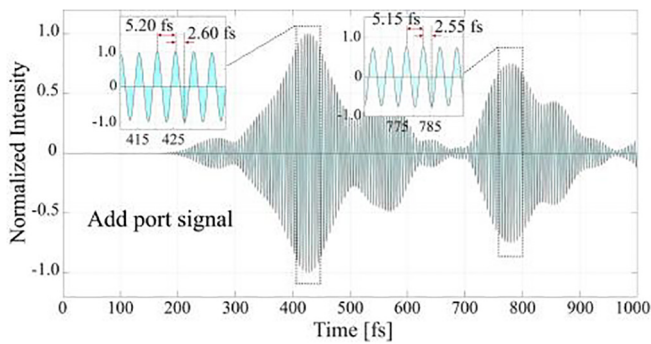


Fig. 3. The simulation results of the reflected polariton at the add port, where the reflected coefficient is 0.9, the oscillation times of ~ 2.6 and 2.55 fs of the 1st and 2nd round filtering are obtained, respectively. The input power is 50 mW.

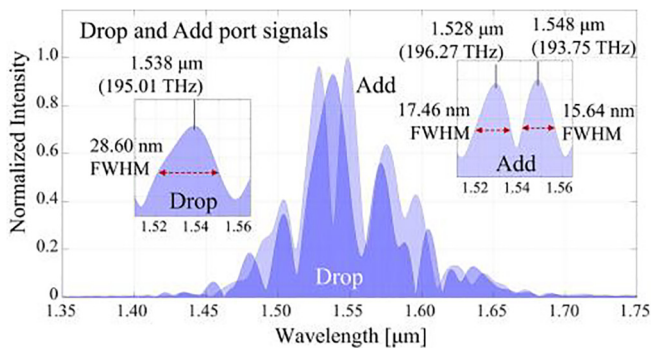


Fig. 4. The simulation results of the polariton in terms of wavelength (frequencies) of the two-level system are obtained at the drop and add ports. The ground and excited state frequencies of the add port are 193.75 and 196.27 THz, respectively. The input power is 50 mW.

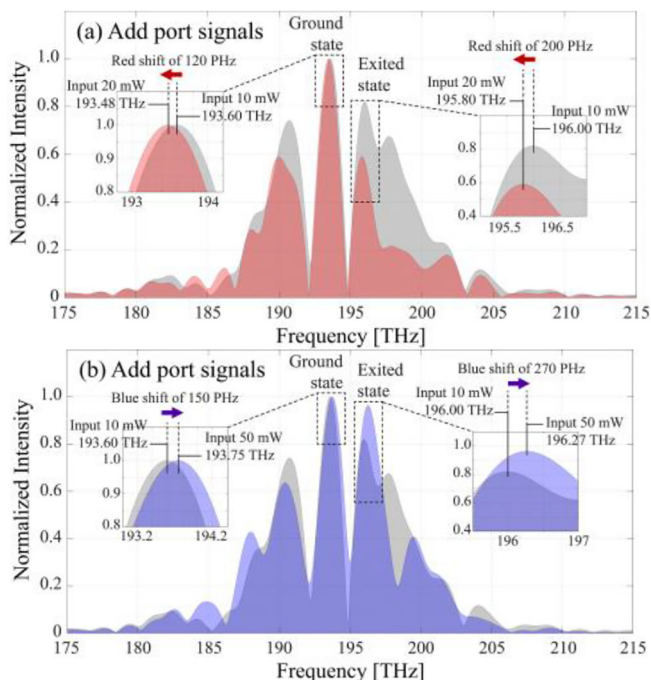


Fig. 5. The simulation results of the system with the same parameters of Fig. 2. The selected input light power are 10 and 50 mW, from which the shift in output frequencies are obtained, where (a) the red shift signals when the input light power is 20 mW, (b) the blue shift signals when input light power is 50 mW. (For interpretation of the references to colour in this figure legend, the reader is referred to the web version of this article.)

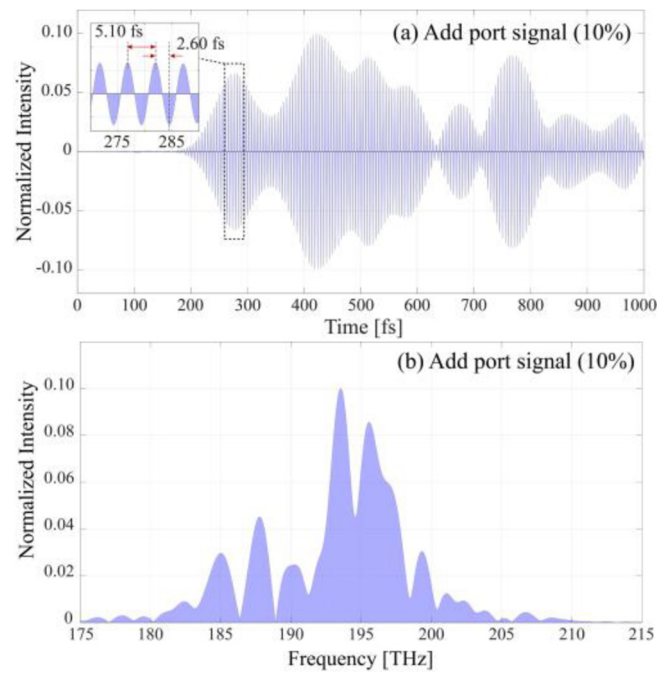


Fig. 6. The results of the two round polariton successive filtering output with the 0.1 transmittance at the add port, where (a) the oscillation pulse width is ~ 2.6 fs, (b) the tunable frequencies from 180 to 210 THz can be obtained. The input power is 50 mW.

light power is 10 and 50 mW, from which the output frequencies can be tuned and obtained, where (a) the redshift signals when the input light power is 20 mW, (b) the blue shift signals when input light power is 50 mW. The results of the two round polariton successive filtering output with the 0.1 transmittances at the add port are shown in Fig. 6, where (a) the oscillation pulse width is ~ 2.6 fs, (b) the tunable frequencies from 180 to 210 THz can be obtained. The blue and red shift results are shown in Fig. 5. The tunable polaritons are obtained and shown in Fig. 6.

We have successfully demonstrated that the meditation characteristics can be described using the polariton successively filtered within the on-chip microring circuit. The device scale and parameters were selected based on the current fabrication technology [11]. By using the selected light source, device scale and parameters, the obtained successive polariton output has shown the interesting results. In which the change in time of 0.045 fs of the 2nd successively filtered signal is obtained. The discrete polariton tunable frequencies of the two-level system are 180–105 THz. In applications, the more successive filtering rounds can be applied, from which results of the switching time will be shorter and shorter, which will be approaching the polariton stopping and blue shift conditions. These can be used to explain the human meditation characteristics, where the states such as the aura, cold body, superpower and fine spiritual signal frequency can be distinguished and described [17]. Moreover, the output polariton characteristics may be useful for the humanoid robotic application, especially, for the humanoid robotic ethics requirement may be possibly applied. The nutrient or substance can be added into the system via the liquid core waveguide, which will be injected and flown by the artificial heart pumping power. The information can be input/output from the system by the plasmonic waveguide (layer).

Acknowledgments

The authors would like to give the appreciation for the research financial support and the research facilities and financial support from the Universiti Teknologi Malaysia, Johor Bahru, Malaysia through

Flagship UTM shine project (03G82), Tier 1 (16H44) and Tier 2 (15J57) grants.

Appendix A. Supplementary data

Supplementary data to this article can be found online at <https://doi.org/10.1016/j.rinp.2018.09.021>.

References

- [1] Gupta P, Ramakrishna SA, Wanare H. Strong coupling of surface plasmon resonances to molecules on a gold grating. *J Optics* 2016;18:105001.
- [2] Florjaczek M, Tremblay R. Strong coupling in grating-assisted multi-waveguide systems. *Optics Commun* 1992;89:385–8.
- [3] Lim HT, Togan E, Kroner M, Sanchez JM, Imamoğlu A. Electrically tunable artificial gauge potential for polaritons. *Nature Comm* 2017;8:14540.
- [4] Matsuura H, Wasaki K. Quantization of artificial neurons: quantum current, model of polariton on axon. *Int J Innovative Comput, Inf Control* 2014;10:1121–33.
- [5] Matsuura H, Wasaki K. Model of polariton, quantum neuron, its network and quantum information. 26th Annual conference of the Japanese Society for AI. 2012.
- [6] Matsuura H, Wasaki K. Quantum theory of fundamental network (path integral expression circuits and network's quantization). *Int J Innovative Comput, Inf Control* 2014;10:1601–23.
- [7] Hagan S, Hirafuji M. The interface in a mixed quantum/classical model of brain function. In: Hameroff SR, Kaszniak AW, Chalmers DJ, editors. *Toward a Science of Consciousness III: The third Tucson Discussions and Debates*. Cambr. MA: MIT Press; 1999.
- [8] Poznanski RR, Cacha LA, Al-Wesabi YMS, Ali J, Bahadoran M, Yupapin PP, et al. Solitonic conduction of electronic signals in the neuronal branchlets with polarized microstructure. *Sci Rep* 2017;7:10675.
- [9] Pornsuwancharoen N, Youplao P, Amiri IS, Ali J, Poznanski RR, Chaiwong K, et al. On-chip polariton generation using an embedded nanograting microring circuit. *Results Phys* 2018;1–4. in press.
- [10] Youplao P, Pornsuwancharoen N, Amiri IS, Jalil MA, Aziz MS, Ali J, et al. Microring stereo sensor model using Kerr-Vernier effect for bio-cell sensor and communication. *NANOCOMMUN NETWORKS* 2018;17:30–5.
- [11] Phatharacorn P, Chiangga S, Yupapin P. Analytical and simulation results of a triple micro whispering gallery mode probe system for a 3D blood flow rate sensor. *Appl Opt* 2016;55:9504–13.
- [12] Atabaki AH, Moazenni S, Pavanello F, et al. Integrating photonics with silicon nanoelectronics for next generation of system on a chip. *Nature* 2018;556:349–54.
- [13] Pornsuwancharoen N, Jalil MA, Amiri IS, Al J, Yupapin P. Dual mode grating sensor using microring conjugate mirror and plasmonic island. *Microwave Opt Technol Lett* 2018. in press.
- [14] Smektala F, Quemard C, Leneindre L, Lucas J, Barthélémy A, De Angelis C. Chalcogenide glasses with large non-linear refractive indices. *J. Non-Cryst Solids* 1998;239:139–42.
- [15] Jomtarak R, Yupapin PP. Transmission characteristics of optical pulse in nested nonlinear microring resonators and gratings. *JOSA B* 2014;31:474–7.
- [16] Yupapin PP, Pornsuwancharoen N. Proposed nonlinear microring resonator arrangement for stopping and storing light. *IEEE Photon Techn Lett* 2009;21:404–6.
- [17] Punthawanunt S, Yupapin P. Meditation on a daily basis makes wise without violence. *J Yoga Phys* 2018;4:555631.